12th Optoelectronics and Communications Conference/16th International Conference on Integrated Optics and Optical Fiber Communication (OECC/IOOC2007)
Technical Digest, July 2007, Pacifico Yokohama

13D1-3

Short-cavity DBR Laser using an InP/InGaAsP Deep-ridge Waveguide with Vertical-groove Gratings

Toru Segawa (1), Boudewijn Docter (1, 2), Takaaki Kakitsuka (1), Shinji Matsuo (1), Tetsuyoshi Ishii (1), Yoshihiro Kawaguchi (1), Yasuhiro Kondo (1), Fouad Karouta (2), Meint K. Smit (2) , and Hiroyuki Suzuki (1)

[1] NTT Photonics Laboratories, NTT Corporation, 3-1 Morinosato Wakamiya, Atsugi, Kanagawa, 243-0198, Japan,
[2] COBRA Research Institute, Technical University of Eindhoven, P.O.Box 127, 5600 MB Eindhoven, The Netherlands,
Tel: +81-46-240-3214, Fax: +81-46-240-3259, e-mail: segawa@aecl.ntt.co.jp

Abstract

A compact distributed Bragg reflector (DBR) laser was fabricated using an InP/InGaAsP deep-ridge waveguide with vertical-groove gratings. We achieved stable single-mode laser operation with an active length of only 25-μm with a low threshold current.

1 Introduction

Large-scale photonic integrated circuits (PICs) are important for future optical networks, because they can provide low-cost, compact, and low-power consumption high-functionality devices through the monolithic integration of many photonic components on a single wafer. In large-scale PICs, short-cavity DBR lasers will be key components: the lasers could be employed as various functional light sources with a small structure, such as a mode-hop-free tunable laser [1] or a high-speed direct modulation laser because of its short-cavity length [2]. For application in large-scale PICs, these lasers should be compact, low power consumption, and easy to integrate.

In this paper, we present short-cavity DBR lasers using an InP/InGaAsP deep-ridge waveguide with vertical-groove gratings, where a corrugation is applied on both sides of the waveguide. This structure enables us to fabricate DBRs with a simple one-step-etching technique [3]. In this structure, the coupling strength is controlled by electron beam (EB) lithography. Various types of DBR lasers can therefore be integrated on a single chip. For example, unidirectional light output from DBR lasers, which is desirable in large-scale PICs, can be achieved by using an asymmetric-κ DBR structure [4]. In addition, high coupling strengths can be obtained with vertical-groove gratings, allowing us to make the device compact. Furthermore, the grating can easily be integrated with other components, such as AWGs, because all these components can be fabricated using the same process. A fabricated device with an active area of only 25 μm and a total device length of 200 μm shows stable laser operation. The threshold current is 13 mA and the side mode suppression ratio (SMSR) is more than 35 dB.

2 Device structure and fabrication

A schematic top view and a photograph of the fabricated device are shown in Fig. 1. The device consists of an active region and front/rear gratings, which are connected by a tapered waveguide. A deep-ridge waveguide structure was used in the grating and tapered waveguide, whereas a shallow-ridge waveguide was used in the active region. The active region consists of a multiple quantum well (MQW) active layer containing 10 QWs on an n-InP substrate. The grating and tapered waveguide regions (InGaAsP layer, λ_{PL} = 1.4Q) were butt-jointed to the active region using selective area growth. Then, a 1.5 μm-thick p-InP cladding layer and a p^+-InGaAsP contact layer were grown over the entire surface. All layers were grown by metal organic vapor phase epitaxy (MOVPE).

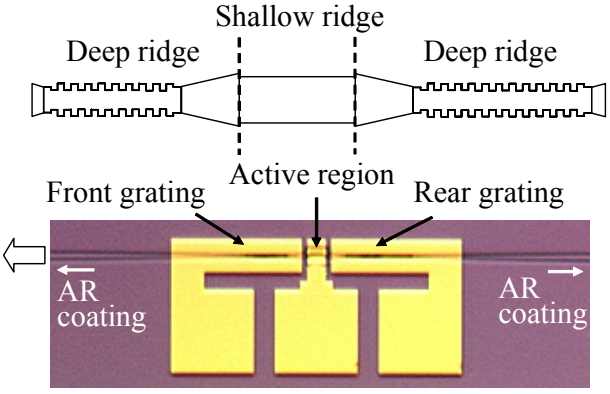

Fig. 1. Schematic top view and photograph of a short-cavity DBR laser.

The deep-ridge, containing the vertical-groove grating structures, was formed by chlorine-based inductively coupled plasma reactive ion etching (ICP-RIE). The waveguide pattern was defined by EB lithography and then transferred into a predeposited SiN layer (600 nm) by RIE, which served as a mask for ICP-RIE. This process provides a deep etch (4 μm) with steep and smooth sidewalls. After fabricating the deep-ridge structure, the shallow-ridge was formed by selective wet etching with diluted HCl, which stops at the top of the active layer. The shallow-ridge waveguide was made 3-μm wide to provide enough gain for the short cavity. The structure was coated with a benzocyclobutene (BCB) and etched back for planarization. Then, Ni/Zn/Au electrodes were deposited on the contact layer by the lift-off process. After the metallization, the sample was cleaved and both facets were coated with antireflection films.

The deep-ridge waveguide with vertical-grove

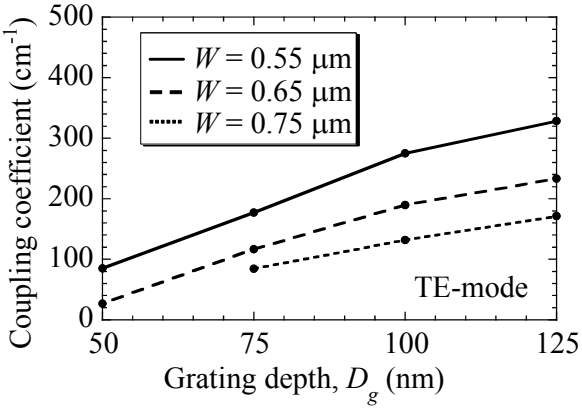

Fig. 2. Measured coupling coefficient.

gratings enables us to obtain a high reflectivity with a small grating length. Figure 2 shows the measured coupling coefficient κ of the fabricated deep-ridge waveguide with vertical-grove gratings as a function of grating depth D_g for the TE mode. We estimated κ by fitting the calculated 3-dB transmission bandwidth with the measured bandwidth of a fabricated grating with a length of 400 μm. For a given D_g, as the waveguide width becomes narrower, κ increases as shown in Fig. 2. Also, as D_g increases, κ increases linearly up to about 330 cm^{-1} for a waveguide width of 0.55 μm. This is adequate to obtain a high reflectivity with a short grating length and thus to reduce the total device size. In the fabricated short-cavity laser, the deep-ridge waveguide is 0.55-μm-wide with 125-nm grating depth. The length of the front and rear gratings are 50 and 80 μm, respectively, which correspond to an estimated peak reflectivity of 84% for the front grating and 95% for the rear grating.

The front/rear gratings need to be connected to the shallow-ridge waveguide, but the mode profiles of the two types of waveguides are different. Modal overlap calculations showed that the optimal shallow-deep transition was obtained when the deep-ridge waveguide was 0.4-μm wider than the shallow-ridge waveguide at the junction. Also, some measurements showed that a tapered waveguide shorter than 23 μm would cause excess loss. We thus used 23-μm long tapered waveguides with a linearly varying width from 0.55 to 3.4 μm. With these tapered waveguides, the total length of the smallest device became 200 μm.

3 Device Characteristics

The L-I curves for the lasers with three different active-region lengths were measured at room temperature as shown in Fig. 3. The measured data includes the fiber-chip coupling losses of 4 dB. The devices show threshold currents of 14, 13 and 10 mA for active region length L_a of 25, 35 and 50-μm, respectively. The power consumption was on the order of 30 mW per device. Despite a few kinks in the L-I curve for the longest device (L_a = 50 μm), lasing output was achieved down to a 25-μm-long active region. Figure 4 shows the lasing spectrum of the smallest device (L_a = 25 μm). We observed a mode spacing of 2.95 nm and a SMSR of 35 dB for the smallest device. For the longer devices, the

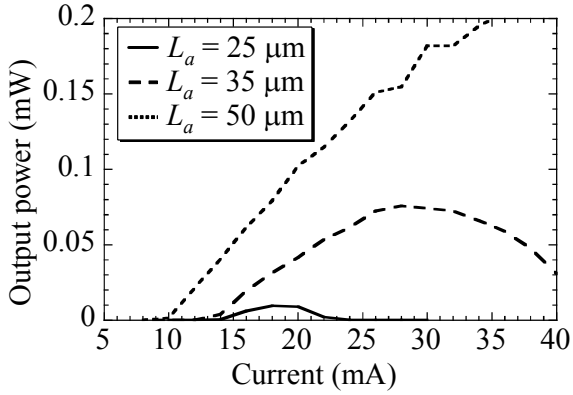

Fig. 3. L-I curves for three short-cavity DBR lasers with active area lengths of 25, 35, and 50 μm.

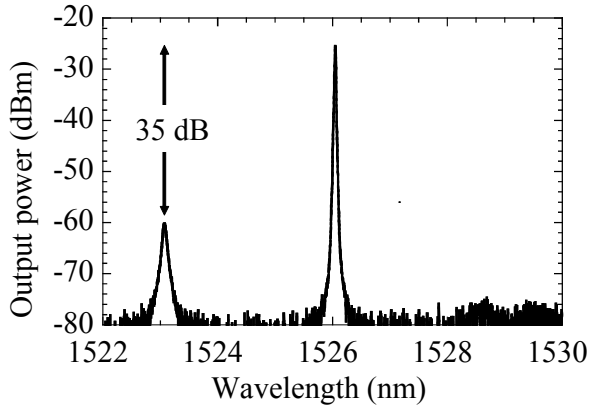

Fig. 4. Laser spectrum of a 25-μm active area short-cavity DBR laser. Drive current was 18 mA.

SMSR was even higher. The high SMSR is attributed to its short cavity length, that is, the large mode spacing, because the reflection spectra of DBRs are relatively broad due to the high coupling coefficient κ of the vertical-grove gratings, and because the single-mode laser operation must be achieved only when enough threshold gain difference occurs in competing modes. Therefore, shortening the lasers cavity by using the high coupling coefficient of vertical-groove gratings is a good approach to the single-mode laser operation of DBR lasers.

4 Conclusion

We presented compact short-cavity DBR lasers using an InP/InGaAsP deep-ridge waveguide with vertical-groove gratings, which makes the devices useful as building blocks in PICs. Devices with an active region of only 25 μm showed single-mode laser operation with a high SMSR. The power consumption was on the order of 30 mW per device, which means that several hundred devices could easily be integrated on a single chip. These devices are promising components for future large scale PICs.

References

1. N. Fujiwara et al., *IEEE JST*QE, **9**, (5), 1132-1137, 2003.
2. M. Aoki et al., *ECOC 2005*, Tu 4. 5. 1, 2005.
3. T. Segawa et al., *IEEE PTL*, **17**, (1), 139-141, 2005.
4. K. Takahata et al., *IEEE JQE*, **30**, (5), 1219-1226, 1994.